

FAR INFRARED EMISSION FROM ELLIPTICAL GALAXIES: NGC 4649, NGC 4472, AND NGC 4636

P. Temi^{1,2}, William G. Mathews³, Fabrizio Brighenti^{3,4} and J.D. Bregman¹

¹Astrophysics Branch, Nasa/Ames Research Center, MS 245-6, Moffett Field, CA 94035

²SETI Institute, Mountain View, CA 94043

³University of California Observatories/Lick Observatory, Board of Studies in Astronomy and Astrophysics, University of California, Santa Cruz, CA 94064

⁴Dipartimento di Astronomia, Universita' di Bologna, via Ranzani 1, Bologna 40127, Italy

ABSTRACT

We present ISOPHOT P32 oversampled maps and P37/39 sparse maps, of three bright elliptical galaxies in the Virgo Cluster. The maps reach the limiting sensitivity of the ISOPHOT instrument at 60, 100, 170 and 200 μ m. Two elliptical galaxies show no emission at all far-IR ISOPHOT wavelengths at a level of few tens of mJy. The null detection provides a test of the evolution of dust in elliptical galaxies and its size distribution and composition. As previous studies have shown, in many elliptical galaxies both IRAS and ISO have detected mid-IR excess 6-15 micron emission relative to the stellar continuum indicating emission from circumstellar dust. Under the assumption that these dusty outflows from evolving red giant stars and planetary nebulae are continuously supplying dust to the interstellar medium, we have computed the infrared luminosity at the ISOPHOT bands appropriate for NGC4472. The null far-IR ISOPHOT observations exceed the far-IR flux expected from dust expelled from a normal old stellar population.

Key words: ISO – Infrared: galaxies – Galaxies: Elliptical – Infrared: ISM – ISM: dust

1. INTRODUCTION

In recent years the traditional view of elliptical galaxies as simple systems of non interacting stars, devoid of interstellar matter, has radically changed. Observations across the electromagnetic spectrum have demonstrated that the interstellar medium (ISM) in elliptical galaxies contains substantial amounts of cold gas and dust in addition to hot gas, the dominant component. Far-IR emission detected by the IRAS satellite and improved optical imaging of elliptical galaxies provide clear evidence for the presence of dust. However, estimates of the total amount of dust, as well as its origin and spatial distribution, remain uncertain and controversial. Optical observations indicate dust masses that are one order of magnitude less than those inferred by IRAS. We have recently embarked on a program to study the infrared emission from early-type galaxies using the large database of observations taken by the ISO satellite. Our principal goals are to observe the spatial location and emission spectrum of dust throughout elliptical

galaxies, and with this information, to determine the origin, evolution, and physical properties of dust in massive elliptical galaxies.

2. OBSERVATIONS AND DATA REDUCTION

ISO provides a vast amount of data with good spatial resolution in the mid and far-IR for a large number of elliptical galaxies. A good fraction of these observations have been taken using ISOPHOT in several observing modes (Astronomical Observing Template), including the oversampled maps P32, the P37/38/39 sparse maps and P22 multi-filter photometry data. Here we present data from three very bright ellipticals located in Virgo Cluster: NGC4649, NGC4472, and NGC4636.

NGC4636 has been observed in the P37/39 AOT mode at 60, 100, and 180 μ m. Observations were made in each filter with one on-source single point staring mode and one off-source exposure. The background position was located $\sim 10'$ north-east from the target, on blank sky position. Data reduction and calibration were performed with the PIA 9.1 package (Gabriel et al. 1997). The reduction included correction for the non linear response of the detectors, readout deglitching, and linear fitting of the signal ramps. After resetting of all ramp slopes and subtracting the dark current, the flux densities were extracted using the power calibration of the reference lamps. After sky subtraction the on-source signal was corrected for the fraction of the point-spread function included within the detector's field of view. A color correction was applied assuming that the SED of the galaxy could be approximated by a blackbody curve with temperature of 30 K. We tested the C100 detector response on a number of galaxies observed in the same observing mode as NGC4636. Integrated fluxes from 8 ellipticals were compared to the IRAS values at 60 and 100 μ m. Calibrated survey scans from the IRAS satellite were extracted using the SCANPI software from IPAC. A very good linear correlation between the ISO and IRAS fluxes is seen at both wavelengths.

NGC4649 and NGC4472 have been observed in P32 mode in three broadband filters at 60, 90 and 180 μ m using the C100 and C200 detectors. The maps were obtained by scanning the spacecraft Y and Z axes in a grid of 4 \times 4 (NGC4649) and 5 \times 4 (NGC4472) points. The focal plane chopper was stepped at intervals of one-third of the detec-

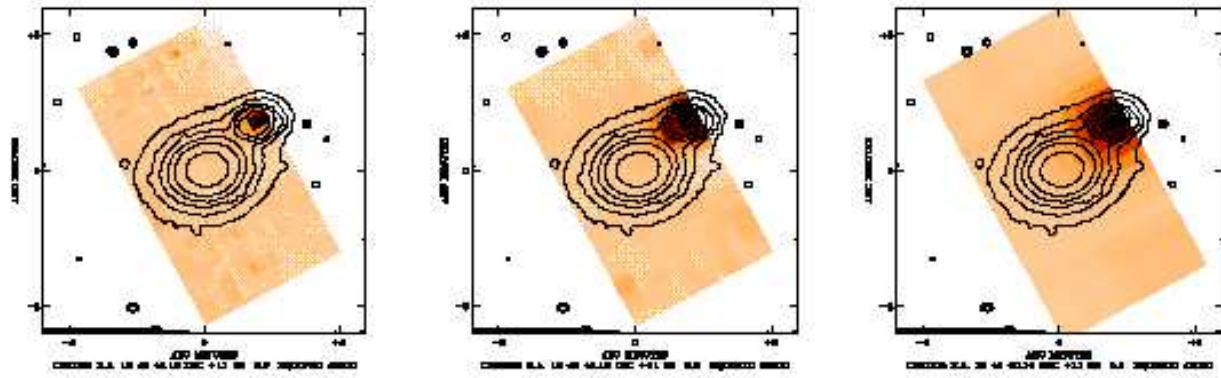


Figure 1. NGC4649 P32 maps at 60, 90, and 180 μm respectively with optical contours superimposed. The galaxy is undetected at all wavelengths observed with ISOPHOT. The bright source at the edge of map is its spiral companion NGC4647 and it is prominent at all three wavelengths. The angular resolution of the oversampled map nicely resolves NGC4647 and shows that there is no contribution from NGC4649 in this aperture centered on the elliptical. At 180 μm the signal from the spiral galaxy extends almost to the location of NGC4649 nucleus, but an analysis of the light profile shows that the emission is clearly coming from the extended far-IR image of NGC4647.

tor pixel, at each raster position, providing a sky sampling in the Y direction of 15" and 30" for the C100 and C200 detectors. To reduce the P32 data we used a dedicated

software package developed at MPI Kernphysik in Heidelberg and supported by the VILSPA ISO Data Center (Tuffs & Gabriel 2002). The new routines allow a proper correction for transients in PHT32 measurements. Both NGC4472 and NGC4649 show no detectable emission at 60, 90, and 180 μm . The maps reach the limiting sensitivity of the ISOPHOT instrument at a level of few tens of mJy and the 3σ upper limits are presented in Table 1. Figure 1 shows the 60, 90, and 180 μm maps for NGC4649. The bright spiral companion NGC4647, recorded at the edge of the maps, is well detected at all three wavelengths and is responsible for the high flux detection, erroneously attributed to NGC4649, reported in literature from IRAS observations. In fact the angular resolution and beam size of the IRAS instruments were not able to disentangle the contribution of the two galaxies. Figure 2 show the 90 μm oversampled map for NGC4472.

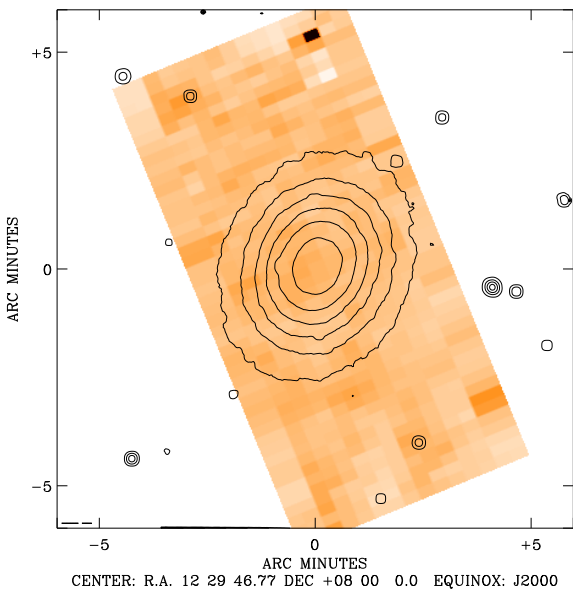


Figure 2. Optical image (contours) superimposed to ISOPHOT 90 μm map for NGC4472. Similar maps at 60 and 180 μm show no detectable emission from the bright elliptical.

Table 1. ISOPHOT flux densities.

	Flux (mJy)		
	NGC4649	NGC4472	NGC4636
$F_{60\mu\text{m}}$	$< 137^c$	$< 147^c$	187 ± 57
$F_{90\mu\text{m}}$	$< 85^c$	$< 99^c$	491 ± 64
$F_{180\mu\text{m}}$	$< 110^c$	$< 87^c$	790 ± 71

^c No detection, 3σ upper limit flux

3. A MODEL FOR NGC4472

Mid-IR (6 - 15 μm) ISO observations of NGC4472 detect strong dust emission that can be understood as emission from circumstellar dust from mass-losing AGB stars at or near the globally expected rate for this galaxy (Athey et al. 2002). Since this dust should emit in the far-IR when it becomes interstellar, it may be significant that NGC4472 is not detected at $\lambda \geq 25\mu\text{m}$ either by ISO or IRAS (Knapp et al. 1989). We now briefly describe an estimate of the far infrared emission from NGC4472, assuming that the grains are dispersed in the hot interstellar gas before sputtering commences. First we calculate the temperature $T_d(r, a)$ of dust grains of radius a (in μm) at galactic radius r and then determine the grain emissivity and luminosity for a distribution of initial grain sizes. Since the 9.7 μm silicate feature is seen in emission in NGC4472, we assume that all grains have properties similar to astronomical silicates (Laor & Draine 1993).

The grain temperature is determined by both absorption of starlight and by electron-grain collisions:

$$\begin{aligned} & \int_0^\infty 4\pi J_*(r, \lambda) Q_{abs}(a, \lambda) \pi a^2 d\lambda + 4\pi a^2 (1/4) n_e \langle v_e E_e \rangle \tau(a) \\ &= 4\pi a^2 \sigma_{SB} T_d(r, a)^4 \langle Q_{abs} \rangle (T_d, a) \end{aligned} \quad (1)$$

although we consider each type of heating separately. The mean intensity of starlight at wavelength λ (in μm) is related to the B-band intensity $J_*(r, \lambda) = J_{\lambda B}(r) \phi(\lambda)$ and the SED $\phi(\lambda)$ taken from Tsai & Mathews (1995). $J_{\lambda B}(r)$ is found by integrating over a de Vaucouleurs stellar profile with a “nuker” core of slope $\rho_* \propto r^{-0.95}$ within $0.031R_e$ (Faber et al. 1997). At a distance $d = 17$ Mpc NGC4472 has an effective radius $R_e = 8.57$ kpc and total stellar mass $M_{*,t} = 7.26 \times 10^{11} M_\odot$ assuming $M_{*,t}/L_B = 9.2$ (van der Marel 1991). The second term on the left represents heating by e^- -grain collisions including a correction $\tau(a)$ for small grains which do not completely stop the electrons (Dwek 1986). For astronomical silicate grains of radius less than $\sim 1\mu\text{m}$ we can use the approximations $Q_{abs} \approx a\psi(\lambda)$ and $\langle Q_{abs} \rangle \approx 1.35 \times 10^{-5} T_d^2 a$. For starlight heating the grain temperature $T_d(r) = 44 J_{\lambda B}^{1/6}$ K is independent of a and varies from 26 K at 1 kpc to 16 K at 10 kpc. For e^- -grain heating the grain temperature $T_d = 0.662(n_e T^{3/2} \tau/a)^{1/6}$ K varies as $a^{-1/6}$ for $a > 0.04\mu\text{m}$ where $\tau \approx 1$ but is independent of grain radius for $a < 0.04\mu\text{m}$ where $\tau \approx 33a$. Figure 3 shows the calculated dust temperature profile for the starlight heating and the e^- -grain heating. For NGC 4472 the collisional heating dominates over the radiative heating for grain sizes $a \lesssim 0.3 \mu\text{m}$.

If grains are expelled from the stars with an initial MRN size distribution

$$S(a, r) = S_o(r) a^{-s}$$

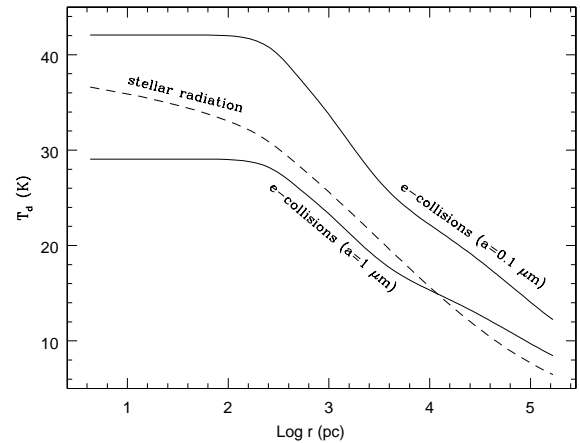


Figure 3. Temperature of dust grains due to starlight heating only (dashed lines), and due to electron-grain collisions only (heavy solid line for grain size $a = 1 \mu\text{m}$; thin solid line for grain size $a = 0.1 \mu\text{m}$). For grains with size $a \lesssim 0.3 \mu\text{m}$ the collisional heating is larger than the radiative one.

where $s = 3.5$ and a is in μm (Mathis et al. 1977), then the steady state grain size distribution in the hot gas is

$$N(r, a) = \left| \frac{da}{dt} \right|^{-1} \frac{S_o(r)}{(s-1)} a^{1-s} \quad a \leq a_{max}. \quad (2)$$

The coefficient

$$S_o(r) = \frac{3\delta\alpha_*\rho_*}{4\pi\rho_g 10^{-12}} \frac{(4-s)}{a_{max}^{4-s}} \quad (3)$$

depends on the rate that the old stellar population ejects mass, $\alpha_* = 4.7 \times 10^{-20} \text{ s}^{-1}$, the initial dust to gas mass ratio scaled to the stellar metal abundance in NGC4472, $\delta = (1/150)z_m(r)$ and the density of silicate grains, $\rho_g = 3.3 \text{ gm cm}^{-3}$. The grain sputtering rate

$$\frac{da}{dt} = -fn_p 3.2 \times 10^{-18} \left[\left(\frac{2 \times 10^6 \text{ K}}{T} \right)^{2.5} + 1 \right]^{-1} \mu\text{m s}^{-1} \quad (4)$$

is a fit to the rate of Draine & Salpeter (1979) with an additional correction $f = f(a, T) \geq 1$ to account for the enhanced (isotropic) sputtering from small grains (Jurac et al. 1998). The hot gas temperature T and proton density n_p for NGC4472 are taken from Brightenti & Mathews (1997).

The infrared emissivity from grains at galactic radius r is

$$\begin{aligned} j(r, \lambda) &= \frac{1}{4\pi} \int_0^{a_{max}} da N(r, a) 4\pi a^2 10^{-8} Q_{abs}(a, \lambda) \\ &\quad \times \pi B(r, a, \lambda) \end{aligned} \quad (5)$$

where $B(T_d(r), a, \lambda)$ is the Planck function.

The total galactic luminosity at wavelength λ is

$$L_\lambda = \int 4\pi j(r, \lambda)(4/3)\pi d(r^3) \quad (6)$$

and the observed flux at λ_μ is

$$F_\nu = 10^{22} \frac{L_\lambda}{4\pi d^2} \frac{\lambda_\mu^2}{c} \text{ mJy.} \quad (7)$$

Figure 4 compares the computed far-IR spectra for the cases of stellar radiation heating and collisional heating with the three ISO flux upper limits. The total IR emission (not shown in the figure) is the sum of the contribution of the two heating sources for each value of a_{max} . Grains with an initial MRN distribution having $a_{max} < 1\mu\text{m}$ are consistent with the null observations of NGC4472 in the far-IR. Grains with radii less than about $0.003\mu\text{m}$ experience stochastic temperature excursions, but this complication should not greatly change our estimated flux in Figure 4.

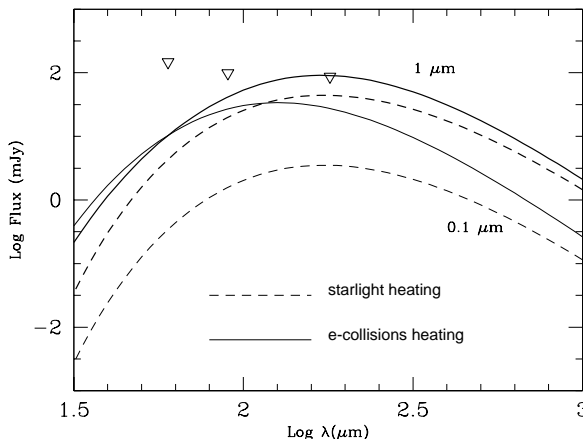


Figure 4. Computed Far-IR flux in mJy from NGC4472 calculated for $a_{max} = 1\mu\text{m}$ (heavy lines) and $a_{max} = 0.1\mu\text{m}$ (light lines). Solid lines show the grain emission based only on electron-grain heating and dashed lines show the emission from grains that are heated only by stellar radiation. The three ISO upper limits are shown with open triangles.

4. RESULTS

We have assumed that the circumstellar dust observed in the mid-IR from NGC4472 (Athey et al. 2002) ultimately

becomes interstellar and is exposed to the mean galactic starlight and to bombardment by thermal electrons in the hot ~ 1 keV gas. Grains receive somewhat more energy from electrons than from stellar photons. The calculated far-IR spectrum peaks at $\lambda \sim 180\mu\text{m}$, a spectral region not accessible to IRAS, but well covered by ISO. However, the computed fluxes are below the observed upper limits if $a \lesssim 0.5\mu\text{m}$. Thus the ISO upper limits do not strongly constrain the properties of dust in NGC4472. We are currently developing a model for the far-IR emission for NGC4636 (Temi et al. 2002). This galaxy shows higher far-IR fluxes (Table 1) and should allow us to put strong constraints on the origin and the evolution of the interstellar dust.

We thank NASA and NSF for grants that funded this research.

REFERENCES

Athey, A., Bregman, J. N., Bregman, J. D., Temi, P. & Sauvage, M. 2002, ApJ 571, 272
 Brighenti, F. & Mathews, W. G. 1997, ApJ, 486, L83
 Draine, B. T. & Salpeter, E. E. 1979, ApJ 231, 77
 Dwek, E. 1986, ApJ 302, 363
 Faber, S. M., Tremaine, S., Ajhar, E. A., Byun, Yong-Lk, Dressler, A., Gebhardt, K., Grillmar, C., Kormendy, J., Lauer, T. R., Richstone, D. 1997, AJ, 114, 1771
 Gabriel, C., Acosta-Pulido, J., Heinrichsen, I., Morriss, H., & Tai, W-M., Astronomical Data Analysis Software and Systems VI, A.S.P. Conference Series, Vol. 125, 1997, Gareth Hunt & H. E. Payne, eds., p. 108.
 Jurac, S., Johnson, R. E., and Donn, B. 1998, ApJ, 503, 247
 Knapp, G. R., Guhathakurta, P., Kim, D-W., Jura, M. A. 1989, ApJS 70,329
 Laor, A. & Draine, B. T. 1993, ApJ, 402, 441
 Mathis, J. S., Rumpl, W., Nordsieck, K. H. 1977, ApJ, 217, 425
 Temi, P., Mathews, W. G., Brighenti, F. and Bregman, J. D. 2002, in preparation
 Tsai, J. C. & Mathews, W. G. 1995, ApJ, 448, 84
 Tuffs, R. J., & Gabriel, C., 2002, In Press.
 van der Marel, R. P., 1991, MNRAS, 253, 710